Coronary Artery–to–Superior Vena Cava Fistula: Contemporary Role of Phonocardiography in Diagnosis

Salman Abdul Basit, MD, Muhammad Sabih Saleem, MD, Muhammad Siddique Pir, MD, Nasir Hamid, MD, Najam Saqib, MD, Christopher Maroules, MD, and Terry Bauch, MD, *Scranton, Pennsylvania; Wilkes-Barre, Pennsylvania; and Norfolk, Virginia*

INTRODUCTION

Coronary arteriovenous fistulae (CAVFs) are rare, congenital low-resistance arteriovenous (AV) connections bypassing the intramyocardial circulation.[1] CAVFs terminating in the superior vena cava (SVC) are the least common variant, representing <2% of cases.[1] We describe a patient with a large CAVF to the SVC, discovered incidentally during atrial fibrillation evaluation and initially suspected to be ruptured sinus of Valsalva aneurysm (SOVA) on transthoracic echocardiography (TTE). Such large CAVFs create hemodynamically significant extracardiac shunts requiring percutaneous or surgical treatment.[2]

CASE PRESENTATION

A 65-year-old patient with hypertension, hyperlipidemia, and a recurrence of basal cell carcinoma underwent preoperative electrocardiography before carcinoma resection. A new diagnosis of atrial fibrillation on electrocardiography led to cardiology consultation. The onset and duration of the atrial fibrillation were unknown. There was no history of chest surgery or trauma. The patient denied symptoms and was physically active walking 3 to 4 miles twice weekly. Blood pressure was 155/80 mm Hg, pulse rate was 106 beats/min (irregular), and peripheral oxygen saturation on room air was normal. The left ventricular (LV) apex felt hyperdynamic, S1 was single and variable with a single S2 and no S3, and a grade III/VI systolic murmur was described at the left sternal border, radiating to the base more than the apex. There was no jugular venous distention or edema, and chest auscultation was clear. Transthoracic point-of-care echophonocardiography revealed abnormal vascular structures anterior to the aortic root and right ventricle, with continuous-wave Doppler flow and associated continuous murmur, suspected to be a ruptured SOVA (Videos 1-4). This point-of-care system includes a unique transthoracic imaging probe with a microphone embedded in the probe surface. The heart sounds detected by the probe are displayed as a phonocardiographic tracing of sound amplitude vs time, below the electrocardiographic tracing. The heart sound audio can also be simultaneously monitored by the sonographer using headphones, and this audio is saved during any cine-loop acquisition. Continuous flow with systolic accentuation of the velocity has been reported (maximum velocity 300 cm/sec).[3] The ability to hear the changing Doppler signal may be of value to sonographers when moving the probe to align optimally with a desired flow.

The aortic valve was trileaflet with mild sclerosis and mild central aortic regurgitation, (vena contracta width 0.18 cm, jet width–to–LV outflow tract width ratio 8%). No significant mitral or tricuspid regurgitation was detected. The single-plane apical four-chamber LV ejection fraction (LVEF) was normal at 64% using Simpson's method (Table 1). There was moderate LV enlargement (100 mL/m^2), and the right ventricle was dilated (basal diameter 4.5 cm). There was severe biatrial enlargement (left atrial [LA] volume index 52 mL/m^2, right atrial volume index 86 mL/m^2). LA reservoir strain was measured using two-dimensional speckle-tracking TTE in the apical four-chamber view and was reduced at 13%.

Cardiac computed tomography (CCT) showed aortic root dilatation of 3.7 × 3.9 × 4.1 cm at the sinuses of Valsalva, along with right coronary artery (RCA) tortuosity and proximal RCA dilatation up to 2.3 cm in diameter, with a proximal RCA-to-SVC fistula (Figures 1 and 2, Video 5). The patient was referred for right and left heart catheterization to assess the hemodynamic significance of the fistula flow and confirm the fistula anatomy. Upon precatheterization physical examination, the murmur was appreciated to be continuous, with systolic accentuation and a subtle increase in systolic intensity following longer cardiac cycle lengths (Audio Clip 1, and https://app.ekodevices.com/recording/c50731a1-4b59-4546-a68b-bd2e19126a84). Coronary angiography and aortic root aortography confirmed proximal RCA dilation with a large fistula draining into the SVC (Figure 3, Video 6). Calibrated levo-phase digital subtraction processing during aortography (Video 6) revealed LV dilation (end-diastolic volume 242 mL) with a lower limit of normal LVEF (55%) and elevated angiographic cardiac output (11.3 L/min; Tables 1 and 2). The left coronary arteries were normal, and collateral vessels were seen from the atrial recurrent branch to the RCA. Left and right heart hemodynamics revealed elevated thermal-dilution cardiac output (10.3 L/min), low systemic vascular resistance (720 dyne/sec/cm^{-5}), normal filling pressures, and no resting pulmonary

From The Wright Center for Graduate Medical Education, Scranton, Pennsylvania (S.A.B., M.S.S., M.S.P., N.S.); Geisinger Wyoming Valley Medical Center, Wilkes-Barre, Pennsylvania (N.H.); and Innovation Health Service, Norfolk, Virginia (C.M., T.B.).

Keywords: Coronary artery aneurysm, Coronary artery fistula, Sinus of Valsalva aneurysm, Intracardiac shunt, Extracardiac shunt

Correspondence: Muhammad Sabih Saleem, MD, The Wright Center for Graduate Medical Education, 501 South Washington Avenue, Scranton, PA 18505 (E-mail: *mdsabih92@gmail.com*).

2468-6441
https://doi.org/10.1016/j.case.2024.05.009

VIDEO HIGHLIGHTS

Video 1: Two-dimensional TTE, parasternal long-axis view with and without color flow Doppler and simultaneous phonocardiographic tracing including audio, demonstrates the dilated proximal RCA with associated fistula (*arrow*) with turbulent, continuous flow. The continuous murmur with systolic accentuation can be heard on audio.

Video 2: Two-dimensional TTE, parasternal short-axis view with and without color flow Doppler and simultaneous phonocardiographic tracing including audio, demonstrates the dilated proximal RCA with associated fistula (*arrow*) with turbulent and continuous flow. The continuous murmur with systolic accentuation can be heard on audio.

Video 3: Two-dimensional TTE, parasternal RV inflow view with and without color flow Doppler and simultaneous phonocardiographic tracing including audio, demonstrates the dilated proximal RCA with associated fistula (*orange arrow*) with turbulent and continuous flow. The continuous murmur with systolic accentuation can be heard on audio.

Video 4: Two-dimensional TTE, parasternal short-axis view with continuous-wave Doppler spectrum and simultaneous Doppler audio through the RCA, demonstrates the continuous flow with systolic accentuation.

Video 5: Three-dimensional CCT, color-coded, volume-rendered reconstruction with the left ventricle removed demonstrates the RCA and fistula (*green*), SVC (*purple*), aorta (*yellow*), PA (*dark blue*), left atrium (*light blue*), and right ventricle (*pink*) in right anterior oblique (RAO), anteroposterior (AP) with caudal angulation, and left anterior oblique (LAO) views.

Video 6: Catheter-based proximal aortography, anteroposterior projection with digital subtraction processing demonstrates the brisk flow in the proximal RCA and fistula into the SVC with subsequent filling of the right atrium and right ventricle before demonstrating late contrast within the left atrium and left ventricle.

View the video content online at www.cvcasejournal.com.

hypertension (Table 3). The pulmonary artery (PA) wedge pressure contour (Figure 4) was notable for a large V wave (24 mm Hg). LA compliance was calculated using the ratio of LA reservoir strain to V-wave amplitude and was low at 0.54 (normal range, >3.0).[4] Saturation sampling did not detect intracardiac shunting, but SVC saturation was elevated at 84%, suggesting an extracardiac left-to-right shunt. The similar thermal-dilution and angiographic cardiac outputs suggested a normal ratio of pulmonary flow (Qp) to systemic flow (Qs) ratio near 1:1. Subsequent cardiovascular magnetic resonance (CMR) revealed left-to-right shunting with a Qp/Qs ratio of 2:1 by the phase-contrast method, which was discordant with a Qp/Qs ratio of 1:1 by the volumetric three-dimensional (3D) CMR method. CMR also identified biventricular dilation with a mildly reduced LVEF (51%) and a normal right ventricular (RV) ejection fraction of 49% (Table 1). Fistula flow near the site of drainage into the SVC was 68 mL/beat by CMR phase contrast (Figure 5) and 71 mL/beat by TTE (Figure 6). Given the findings of a large fistula, high-output state, cardiac remodeling, and atrial fibrillation, a surgical unroofing and closure of the fistula along with bypass grafting of the RCA was recommended, but has not yet been performed.

Table 1 Chamber dimensions

	LVEDV, mL	LVESV, mL	LVEF, %	RVEF, %
TTE	189	68	64	
CMR	241	120	51	49
CATH	242	109	55	

Volumes were obtained from calibrated catheter-based digital subtraction angiography using a single-plane method. Volumes obtained on nonenhanced TTE were measured using the single-plane Simpson's method during atrial fibrillation using the average of two cardiac cycles. Volumes from CMR used a conventional functional short-axis cine stack.
CATH, catheter-based angiography; *LVEDV*, LV end-diastolic volume; *LVEF*, LV ejection fraction; *LVESV*, LV end-systolic volume; *RVEF*, RV ejection fraction.

DISCUSSION

We describe an asymptomatic patient presenting with atrial fibrillation and a continuous systolic murmur, with a large RCA-to-SVC fistula on imaging, leading to chronic extracardiac shunting from systemic artery (proximal RCA) to systemic vein (SVC) and equally elevated stroke volumes from the right and left ventricles, associated with dilation of both atria and ventricles.

CAVFs were first reported in 1865 by Krause.[1] Their prevalence is 0.002%,[1] and they account for nearly 50% of coronary artery anomalies. Almost 90% of CAVFs are congenital, but they can be acquired. At the time of embryogenesis, fistulous connections may develop between the coronary arteries and any heart chamber or vessel. Failure to later fuse these connections results in congenital CAVF. Acquired CAVFs are rare and can result from cardiac trauma, radiation therapy, complications during coronary bypass surgery, or coronary diseases such as vasculitis.[2] Asymptomatic patients are usually diagnosed incidentally while undergoing coronary angiography.[1] As age increases, they may become symptomatic.[1] A large fistula may present with ischemic symptoms or with symptoms of high-output heart failure such as dyspnea, pedal edema, and orthopnea. A CAVF can be confused with other conditions that may cause coronary dilation and a continuous murmur such as ruptured SOVA, patent ductus arteriosus, systemic AV fistula, pulmonary AV fistula, anomalous origin of the left coronary artery from the PA, aortopulmonary window, and internal mammary artery–to–PA fistula.[1] Our case is an example in which transthoracic echocardiographic features of large proximal coronary fistulae may be confused with a ruptured SOVA given the presence of elevated periaortic systolic and diastolic flow in both pathologies.[5] Multimodality imaging is indicated to confirm the diagnosis of CAVF and to identify the origin, size, course, and termination of the fistula.[2] CCT and catheter-based angiography can identify the anatomy; however, CCT has the advantage of 3D analysis, which aids planning for percutaneous or surgical closure. Catheter-based angiography may have quality limitations when fistula flow is higher than coronary flow, and opacification of the native coronary arteries may be inadequate, as occurred in our case. CMR can perform 3D

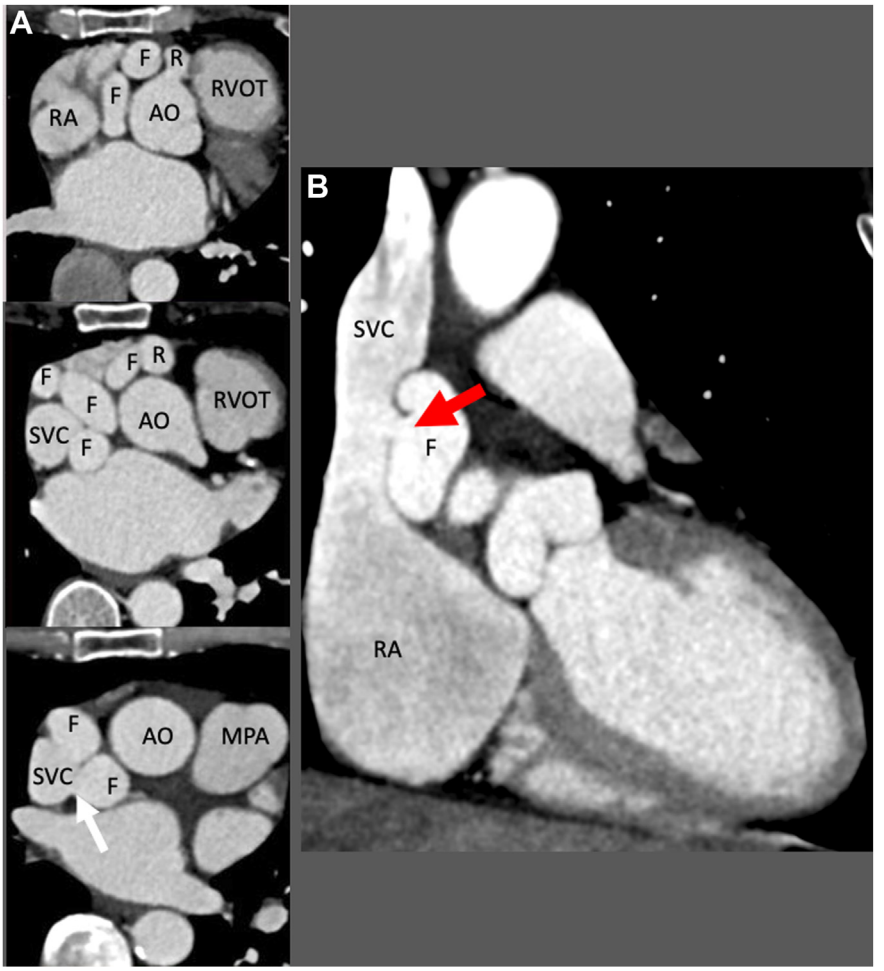

Figure 1 CCT, multiplanar axial reconstructions, inferior to superior display **(A)** demonstrates the RCA (R) origin from the aorta (AO) in a normal anterior location and the adjacent fistula (F), right atrium (RA), right ventricular outflow tract (RVOT), and SVC. The bottom image demonstrates the fistula draining into the SVC (*white arrow*). The coronal display **(B)** demonstrates the SVC-to-RA fistula (*red arrow*). *MPA*, Main PA.

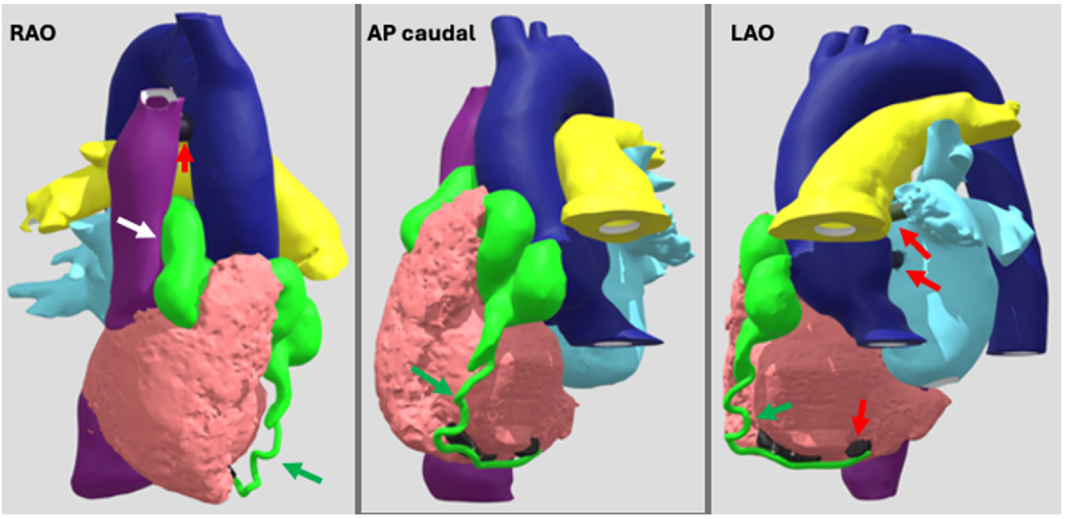

Figure 2 CCT, 3D color-coded volume-rendered reconstruction with the left ventricle removed, right anterior oblique (RAO) view, anteroposterior (AP) with caudal angulation, and left anterior oblique (LAO) view displays demonstrate the middle segment of the RCA (*green arrows*) and fistula (*green*), SVC (*purple*), aorta (*yellow*), PA (*dark blue*), left atrium (*light blue*), and right ventricle (*pink*). The site of fistula drainage into SVC (*white arrow*) is shown. Note that there are artificial support structures (*black*) added to the model for future 3D printing (*red arrows*). An interactive model is available at https://skfb.ly/oHJEQ.

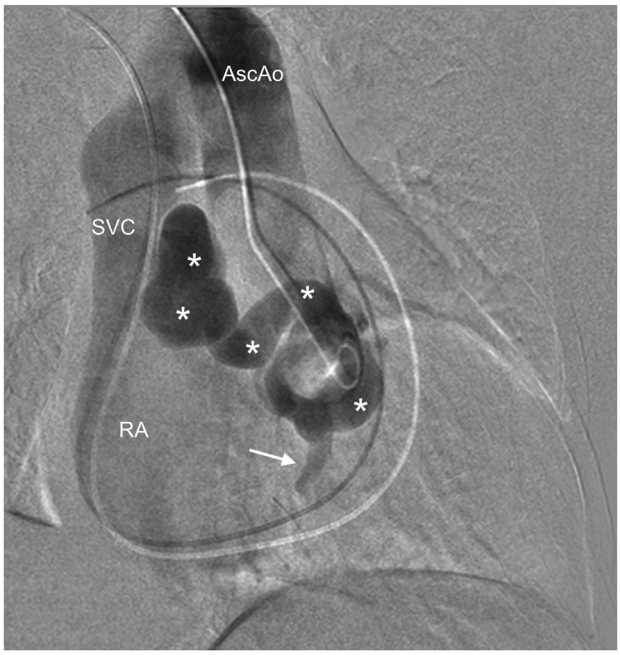

Figure 3 Catheter-based proximal aortography with digital subtraction angiography, anteroposterior view, demonstrates the right atrium (RA), ascending aorta (Asc Ao), SVC, and fistula from the RCA (*asterisk*) with a partially visualized proximal RCA (*arrow*).

Table 2 Net forward flow data (milliliters per beat) by location and modality

	MPA	LVOT	Fistula	Asc AO	SVC	Desc AO
CMR-PC	133		68	56	21	34
CMR-volumetric	116 (RV)	121 (LV)				
TTE-PW	130	115	71			
TTE-2D		122 (LV)				
CATH-TD	121					
CATH-FICK		125		68		
CATH (TD-FICK)			53			
CATH-LVG		133				

Asc AO, Ascending aorta; *CATH-FICK*, direct Fick's method cardiac output (using SVC saturation to measure ascending aortic flow and PA saturation to measure LVOT flow); *CATH-LVG*, left ventriculography; *CATH-TD*, thermal dilution; *CATH-TD-FICK*, indirect estimation of fistula flow using difference between CATH-TD and CATH-FICK measurements; *CMR-PC*, phase-contrast CMR; *Desc AO*, descending aorta; *LVOT*, LV outflow tract and flow through the aortic valve; *MPA*, main PA; *TTE-2D*, LV volumes measured using the single-plane Simpson's method on a nonenhanced four-chamber view during atrial fibrillation using the average of two cardiac cycles; *TTE-PW*, pulsed-wave Doppler.

Table 3 Invasive hemodynamic data

	IVC	SVC	RA	RV	PA	PW	LA	LV	AO
Saturation, %	73	84	87	85	87		99		99
Pressure, mm Hg			—/2/1		30/8/18	—/24/9	—/28/10	140/4	136/61/95

Pressures are mean or systolic/diastolic/mean or A/V/mean.
AO, Aortic root; *IVC*, inferior vena cava; *LA*, left atrium; *LV*, left ventricle; *PW*, pulmonary wedge; *RA*, right atrium; *RV*, right ventricle.

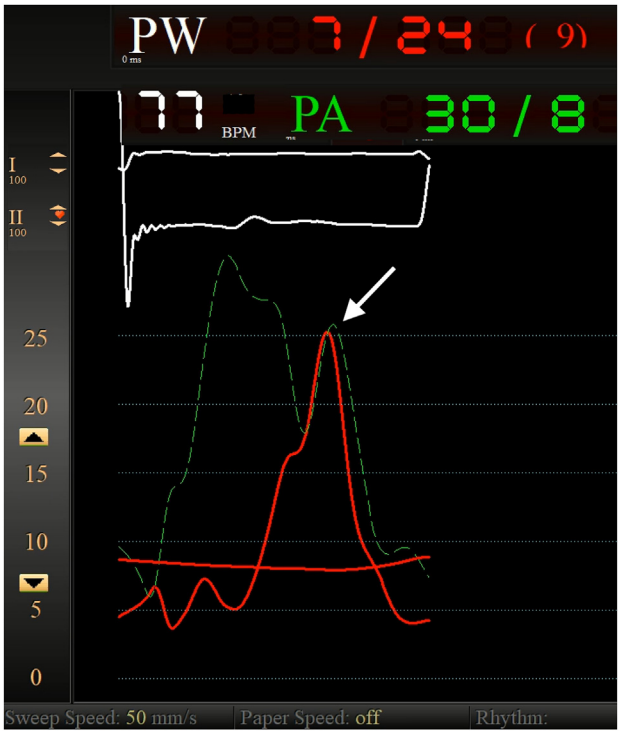

Figure 4 Ensemble-averaged PA (*green*) and PA wedge (PW; *red*) pressure waveforms from right heart catheterization. Large V waves (*arrow*) are present on both waveforms and from an elevated cardiac output with reduced LA chamber compliance.

angiography of the fistula but requires more time and patient cooperation and is more prone to artifacts compared with CCT. CMR does provide other data complementary to CCT, including direct flow measurements in the great vessels and functional analysis of the ventricles. Cardiac catheterization is used to assess intracardiac pressures and quantify shunt flow. The mainstay of treatment is either percutaneous embolization via transcatheter approach or surgery,[1] but few data are available to guide treatment, and recommendations are opinion based. Although precise guidelines for the management of CAVF have not been established, it is recommended that these be percutaneously or surgically treated if causally associated with ischemia or arrhythmia, endarteritis, chamber dilation, or ventricular dysfunction.[6] Asymptomatic patients with small fistulae are monitored for complications. Spontaneous closure occurs in 1% to 2% of cases.[1]

This case reminds us to be vigilant for rare heart diseases when assessing seemingly routine referrals. Recognizing clinical and imaging manifestations of uncommon large CAVF is essential to prevent adverse cardiac remodeling.[7-9] The reconciliation of apparently discordant clinical, imaging, and invasive data can be understood with further consideration of the lesion pathophysiology and the methodology of each diagnostic modality.

The murmur in this case was initially labeled as systolic, likely because of cognitive bias[10] anchoring the listener to the more commonly encountered and louder systolic component of a truly continuous murmur. The spectrographic analysis (Figure 7) confirmed a systolic accentuation of this murmur that may have drawn attention away from the additional diastolic component, and this corresponds to the higher systolic velocity in the RCA as measured by Doppler (Video 4), consistent with current understanding of murmur origins.[11] The holodiastolic component of the murmur occurs during a period lower flow velocity of 140 cm/sec, which is nevertheless greater than normal. The volume of diastolic fistula flow remains significant as well, driven by a pressure gradient from the aortic root to the SVC of ≥60 mm Hg, and contributes to the murmur intensity.

Data from CMR appeared internally discordant given a Qp/Qs ratio of 2:1 by phase-contrast flow but 1:1 by 3D volumetric measurements of LV and RV stroke volumes (Table 2). The 3D volumetric method in CMR involves tracing the endocardial border on 10 to 12 basal to apical short-axis cine slices of the left and right ventricles and combining the data to calculate the volumes in a manner similar to 3D TTE. Comparison of the LV and RV stroke volumes is then used to detect any difference that would indicate the presence of a shunt, or a regurgitant valve lesion. The CMR phase-contrast technique is a two-dimensional flow measurement at a selected location analogous to the measurement of stroke volume using pulsed-wave Doppler. The accuracy of the result depends on the precise location of the sampled flow in both CMR and Doppler methods. Once the stroke volume is measured, it is multiplied by the heart rate to calculate flow (Q) in milliliters per minute. Qp by phase contrast is typically measured in the main PA. Qs by phase contrast is typically measured in the ascending aorta, near the sinotubular junction. Both standard measurement locations were applied during CMR in our patient, so the Qs sample excluded the large shunt flow from the RCA to the SVC that occurred proximal to that sampling location and measured only the remaining flow into the ascending aorta, resulting in falsely low measurement of the total flow coming out of the left ventricle but a correct measurement of the stroke

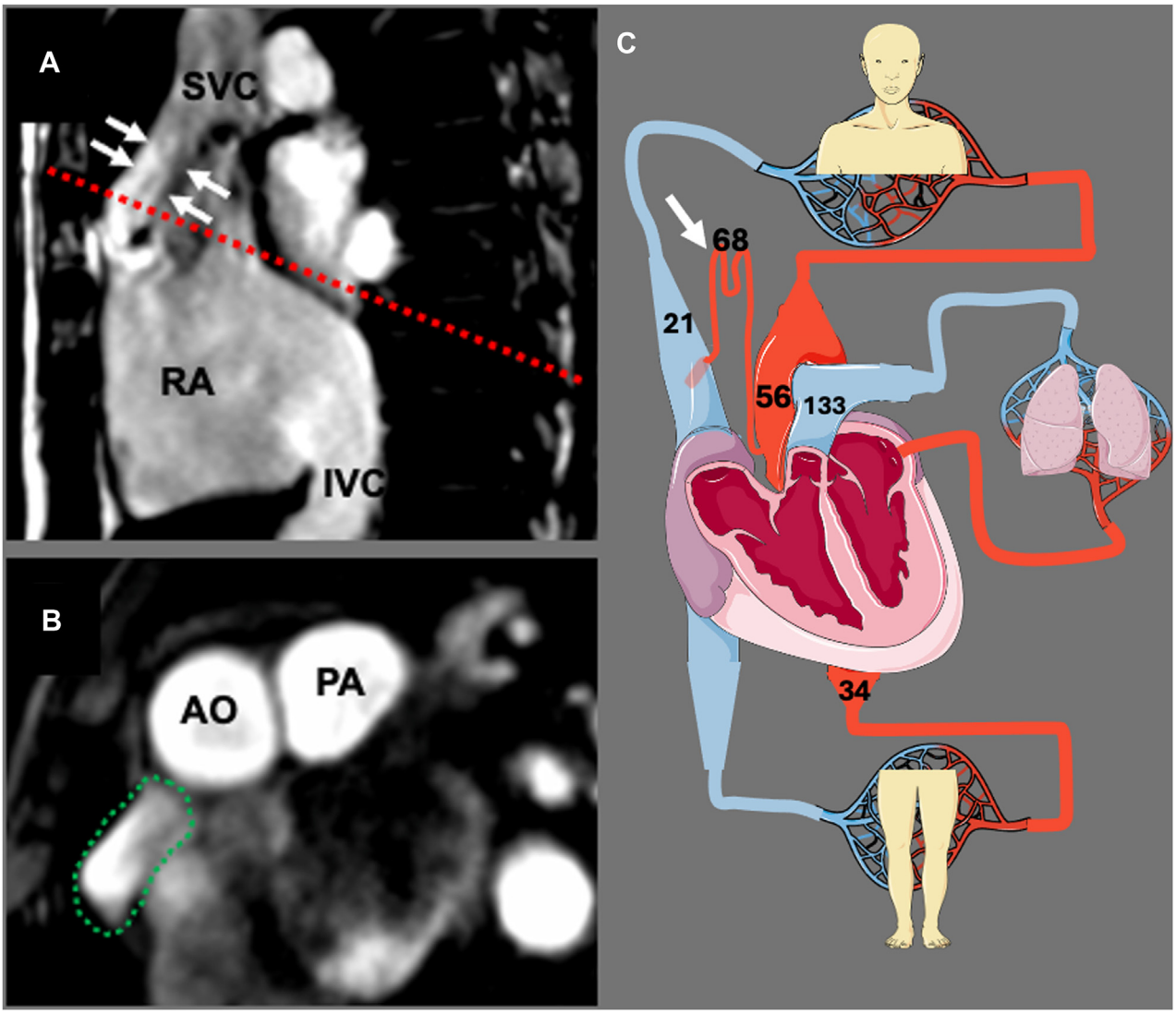

Figure 5 CMR, phase-contrast sequence, sagittal **(A)** display-aligned (*dotted red line*) and oblique axial view **(B)**, demonstrates the fistula (*dotted green circle*) draining into SVC *(white arrows)* and allows quantitation of the fistula flow. An anatomic cartoon of the phase contrast flow measurements at each anatomic location **(C)** demonstrates the findings on CMR: fistula, 68 mL/beat (*white arrow*); SVC proximal to fistula drainage, 21 mL/beat; ascending aorta distal to fistula, 56 mL/beat; main PA, 133 mL/beat; and descending aorta, 34 mL/beat. This figure was partly generated using Servier Medical Art, provided by Servier, licensed under a Creative Commons Attribution 3.0 Unsupported license.

volume into the remainder of the systemic circulation of 56 mL/beat. A direct sampling of fistula flow (Figure 5) measured 68 mL/beat. Thus, the total stroke volume out of the left ventricle by phase contrast was 56 + 68 mL/beat, or 124 ml/beat. This matches the 3D volumetric measurement of 121 mL/beat, demonstrating internal data consistency and excluding significant mitral regurgitation or a ventricular septal defect, as those would cause lower forward flow out of the left ventricle compared with the volumetric stroke volume. RV phase-contrast stroke volume as measured in the main PA was 133 mL/beat, and the 3D volumetric measurement was 116 mL/beat. The difference is believed to reflect minor measurement errors which occur during phase contrast compared with phantom calibrations, as well as known challenges tracing the contours of the trabeculated right ventricle. Essentially, the data for the right ventricle indicate the absence of significant tricuspid regurgitation, and the similar RV and LV stroke volumes by both methods indicate the lack of an intracardiac shunt or patent ductus arteriosus.

This case also illustrates the need to differentiate intra- and extracardiac shunts and understand the variations in types of extracardiac shunts. An intracardiac shunt will cause a difference in forward flow through the pulmonary and aortic valves, but an extracardiac systemic arterial–to–systemic venous shunt will not. An example of an extracardiac systemic artery–to–vein shunt is a surgical AV fistula for dialysis. This commonly encountered shunt creates a low-resistance path for arterial blood to bypass the forearm and return to a systemic vein. An abnormally large dialysis fistula will cause an elevated cardiac output state that affects the left and right heart equally, and Qp/Qs will be 1:1, identical to the flow created by

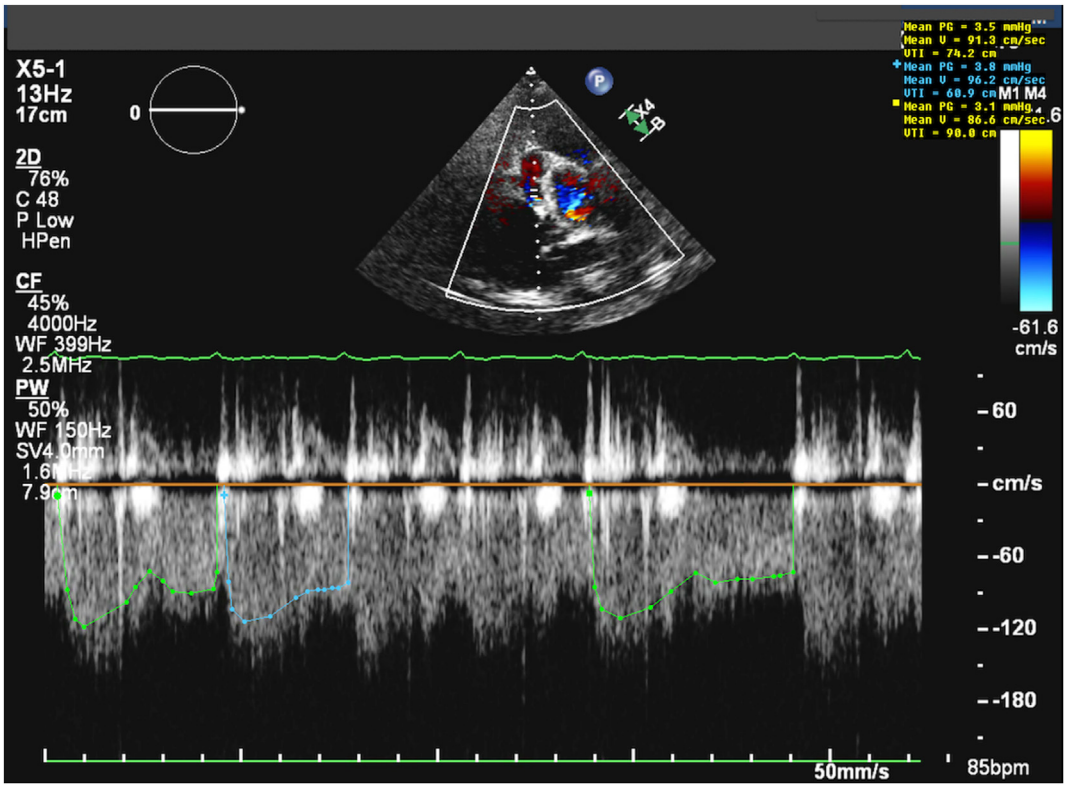

Figure 6 Two-dimensional TTE, modified parasternal basal short-axis view with color flow Doppler-guided pulsed-wave spectrum of the proximal fistula segment, demonstrates continuous flow, and averaging the modal flow velocity–time integral envelopes *(blue and green lines)* calculates a mean velocity-time integral of 75 cm. The fistula diameter at this Doppler measurement site was 1.1 cm, which calculates an estimated flow volume of 71 mL/beat.

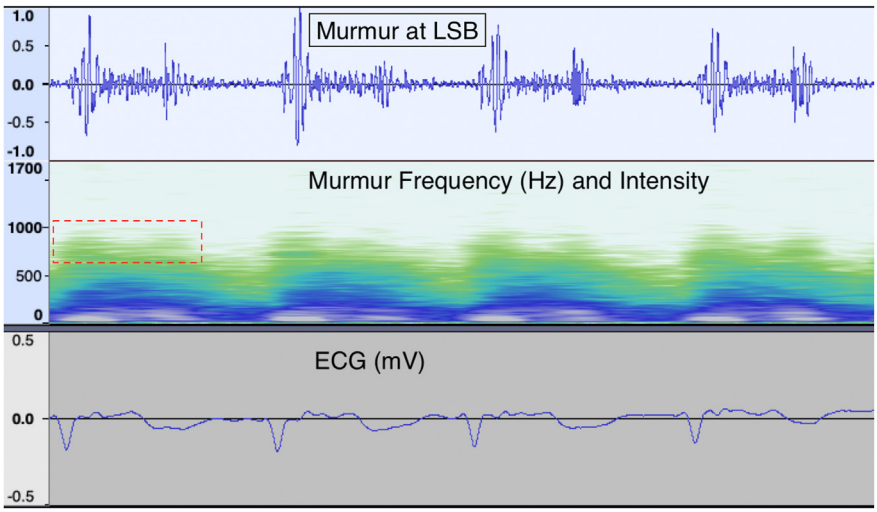

Figure 7 Spectral frequency display of continuous murmur recorded by an electronic stethoscope with a built-in electrocardiographic sensor. *Dotted rectangle* highlights the additional higher frequency sound energy present during systole, which corresponds to the demonstrated increased systolic flow velocity into the fistula. The greater intensity of the *blue/green* region during systole, seen below the *dotted box*, indicates a louder murmur during systole, and it is this systolic accentuation that may result in a false impression of an isolated "systolic" murmur. *LSB*, Left sternal border.

the fistula from a systemic artery (proximal RCA) to a systemic vein (SVC), as demonstrated in our case. A different type of extracardiac shunt occurs when a systemic artery drains into a PA, as in a patent ductus arteriosus. In that anatomy, a portion of the stroke volume from the left ventricle enters the PA and thus returns to the left ventricle but does not add to the filling of the right ventricle. The

result is a higher flow out the aortic valve than out of the pulmonic valve and a higher LV stroke volume compared with the right. The Qp/Qs ratio in this unique case of extracardiac left-to-right shunting will be <1:1, as Qs is higher than Qp.

The invasive hemodynamics were notable for large LA V waves on the PA and PA wedge pressure recordings (Figure 4). This seemed discordant with the lack of significant mitral valve disease by CMR and TTE, but the differential diagnosis for large V wave includes atrial noncompliance and elevated cardiac output, both of which were present in our case and help explain this finding.

We also noted some discordance in the LVEF measurement between CMR (51%) and TTE (64%). The CMR value was considered to be more accurate and recognizes that the higher LVEF from TTE was based on a single-plane view (see Table 1). Given the lack of coronary and valvular heart disease, and no disease-specific pattern of gadolinium enhancement on CMR, we hypothesize that the mild LV dysfunction may have been a result of hypertension, atrial fibrillation of unknown duration, and chronic cardiac remodeling from the large congenital CAVF.

CONCLUSION

Coronary artery–to–SVC fistulae are rare. Echocardiographic features may mimic a ruptured SOVA. CCT should be performed to confirm the diagnosis. Awareness of this uncommon abnormality and the associated physical examination and imaging manifestations can improve recognition and management. Contemporary point-of-care ultrasound with phonocardiography may aid in a timely diagnosis of such disorders and facilitate timely intervention.

ETHICS STATEMENT

The authors declare that the work described has been carried out in accordance with The Code of Ethics of the World Medical Association (Declaration of Helsinki) for experiments involving humans.

CONSENT STATEMENT

The authors declare that since this was a non-interventional, retrospective, observational study utilizing deidentified data, informed consent was not required from the patient under an IRB exemption status.

FUNDING STATEMENT

The authors declare that this report did not receive any specific grant from funding agencies in the public, commercial, or not-for-profit sectors.

DISCLOSURE STATEMENT

The authors report no conflict of interest.

SUPPLEMENTARY DATA

Supplementary data related to this article can be found at https://doi.org/10.1016/j.case.2024.05.009.

REFERENCES

1. Lim JJ, Jung JI, Lee BY, Lee HG. Prevalence and types of coronary artery fistulas detected with coronary CT angiography. AJR Am J Roentgenol 2014;203:W237-43.
2. Shadman S, Gattani R, Bakhshi H, Sidhu BS, Singh R, Emaminia A. Indispensable Role of Multimodality imaging in diagnosis and management of coronary arteriovenous fistulas. JACC Case Rep 2022;4:826-31.
3. Ofili EO, Kern MJ, Labovitz AJ, St Vrain JA, Segal J, Aguirre FV, et al. Analysis of coronary blood flow velocity dynamics in angiographically normal and stenosed arteries before and after endolumen enlargement by angioplasty. J Am Coll Cardiol 1993;21:308-16.
4. Reddy YNV, Obokata M, Egbe A, Yang JH, Pislaru S, Lin G, et al. Left atrial strain and compliance in the diagnostic evaluation of heart failure with preserved ejection fraction. Eur J Heart Fail 2019;21:891-900.
5. Shrivastava V, Akowuah E, Cooper GJ. Coronary artery aneurysm with a fistulous connection to the right atrium mimicking a sinus of Valsalva aneurysm. Heart 2003;89:e4.
6. Al-Hijji M, El Sabbagh A, El Hajj S, AlKhouli M, El Sabawi B, Cabalka A, et al. Coronary artery fistulas: indications, techniques, outcomes, and complications of transcatheter fistula closure. Cardiovasc Interv 2021;14:1393-406.
7. Qureshi SA. Coronary arterial fistulas. Orphanet J Rare Dis 2006;1:51.
8. Stout KK, Daniels CJ, Aboulhosn JA, Bozkurt B, Broberg CS, Colman JM, et al. 2018 AHA/ACC guideline for the management of Adults with congenital heart disease. Circulation 2019;139:e698-800.
9. Warnes CA, Williams RG, Bashore TM, Child JS, Connolly HM, Dearani JA, et al. ACC/AHA 2008 guidelines for the management of Adults with congenital heart disease. Circulation 2008;118:e714-833.
10. Kahneman D. Thinking, Fast and Slow. 1st ed. New York, NY: Farrar, Straus and Giroux; 2011.
11. Murgo JP. Systolic ejection murmurs in the era of modern cardiology: what do we really know? J Am Coll Cardiol 1998;32:1596-602.